

# Synthesis, Characterization, Antioxidant and Antibacterial Activities of Zinc Ferrite and Copper Ferrite Nanoparticles

Kaveh Hatami Kahkesh<sup>1</sup>, Zahra Baghbantaraghdari<sup>2</sup>, Donya Jamaledin<sup>3</sup>, Farnaz Dabbagh Moghaddam<sup>4,\*</sup>, Naoki Kaneko<sup>5,\*</sup>, Mahsa Ghovvati<sup>5,\*</sup>

<sup>1</sup> Department of Basic Medical Science, Faculty of Veterinary Medicine, Shahrekord University, Shahrekord, Iran

<sup>2</sup> Department of Chemical, Materials & Industrial Production Engineering, University of Naples Federico II, Naples, 80125, Italy

<sup>3</sup> Faculty of Veterinary Medicine, Shahid Chamran University of Ahvaz, Ahvaz, Iran

<sup>4</sup> Institute for Photonics and Nanotechnologies, National Research Council, Via Fosso del Cavaliere, 100, 00133, Rome, Italy

<sup>5</sup> Department of Radiological Sciences, David Geffen School of Medicine, University of California Los Angeles, Los Angeles, California, USA

**Corresponding authors:** [farnaz.dabbagh.moghaddam@gmail.com](mailto:farnaz.dabbagh.moghaddam@gmail.com) (F.Dabbagh Moghaddam); [NKaneko@mednet.ucla.edu](mailto:NKaneko@mednet.ucla.edu) (N.Kaneko); [MGhovvati@mednet.ucla.edu](mailto:MGhovvati@mednet.ucla.edu) (M. Ghovvati)



*Mater. Chem. Horizons*, 2023, 2(1), 49-56

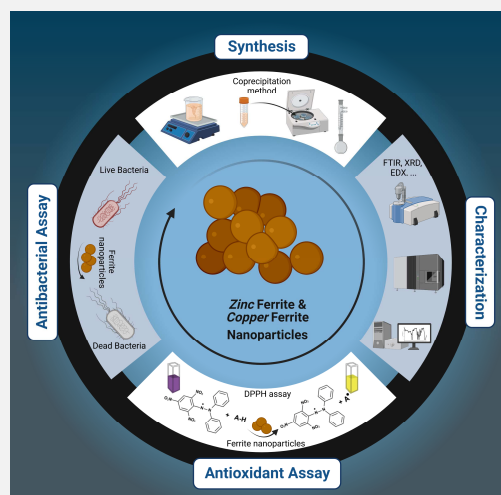


10.22128/MCH.2022.613.1030



## ABSTRACT

Spinel ferrite nanoparticles have drawn the attention of researchers because of their unique properties and promising applications. To date, very little information is available on the biological activity of spinel ferrites. This study used the coprecipitation technique to synthesize copper ferrite ( $\text{CuFe}_2\text{O}_4$ ) and zinc ferrite ( $\text{ZnFe}_2\text{O}_4$ ) nanoparticles to evaluate their antioxidant and antibacterial activities. The nanoparticles were then characterized using Fourier transform infrared spectroscopy, field emission scanning electron microscopy, X-ray diffraction, vibrating-sample magnetometer, and energy dispersive X-Ray analysis. Agar disk diffusion and 2,2-diphenyl-1-picrylhydrazyl hydrate tests were used to measure the antibacterial and antioxidant properties of copper ferrite and zinc ferrite nanoparticles. The antioxidant activity of copper ferrite and zinc ferrite nanoparticles was 71% and 80%, respectively. Additionally, it was shown that nanoparticles made of copper ferrite and zinc ferrite had a strong antibacterial effect on *Escherichia coli* and *Staphylococcus aureus*.



**Keywords:** Magnetic nanoparticles, zinc ferrite, copper ferrite, antioxidant, antibacterial

## 1. Introduction

Nowadays, various nanoparticles have been designed and manufactured with the aim of studies in the field of energy, environment protection, healthcare, drug delivery, and therapy [1-6]. Ferrites, a kind of ferrimagnetic ceramic having the general formula  $\text{MFe}_2\text{O}_4$  (M stands for bivalent metal ions, like Zn, Cu, Ni, Co, Fe, and Mn), are widely recognized for their great chemical stability, electrical resistance, and magnetic and physical characteristics [7, 8]. The garnet, hexagonal, and spinel structures of ferrites are determined by their original crystal lattice. The inverse and normal spinel ferrites are particularly appealing among these structures [7, 8]. Among the ferrites, spinel ferrite has unique qualities like thermal and chemical stability and the dependency of magnetic characteristics on particle size and offers enormous promise in a variety of technical applications, which include magnetic resonance imaging, ferrofluids, and photoinduced trans-former [9]. Due to its numerous bioapplications, such as high-density magnetic recording medium, hyperthermia, and magnetically guided drug administration, magnetic nanoparticles' peculiar structure and magnetic characteristics have increased interest in these materials [10].

The term "spinel ferrite nanoparticles" (SFNPs) refers to metal oxides having a spinel structure and the general formula  $\text{AB}_2\text{O}_4$ , where A and B indicate different metal cations located at tetrahedral (A site) and octahedral (B site)

Received: September 24, 2022

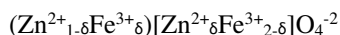
Received in revised: November 12, 2022

Accepted: November 16, 2022

This is an open access article under the [CC BY](https://creativecommons.org/licenses/by/4.0/) license.



sites, respectively, at least with ferric in the chemical formula. Both locations have octahedrally and tetrahedrally coordinated metal cations to oxygen atoms. The types, quantities, and placements of the metal cations in the crystalline structure have a significant impact on the physicochemical characteristics of ferrites [11]. Distinctive magnetic properties such as spin filtering, superparamagnetism, single domain effects, high coercivity, moderate magnetization, etc., are present in nanostructures of magnetic transition oxides of spinel structure  $MFe_2O_4$  ( $M=Mn, Fe, Co, Ni, \text{etc.}$ ), having remarkable biological and industrial functionalities [12]. Typically, there are two types of spinel structures: normal and inverse. In normal spinel, the  $Me^{2+}$  cations are positioned in A sites, and the  $Fe^{3+}$  cations are in B sites. In inverse spinel, the  $Me^{2+}$  cations are in B sites and the  $Fe^{3+}$  cations in both A and B sites, which is depend on the preparation method [13, 14]. The spinel ferrites are described by the formula  $(A)[B]_2O_4$ , where (A) and [B] indicate cations in tetrahedral and octahedral sites of a cubic closest packing of oxygen, respectively. The entirety of the  $Zn^{2+}$  ions are located in the A-sites and the  $Fe^{3+}$  ions are located in the B-sites in bulk zinc ferrite, which exhibits a typical spinel structure. Nevertheless, unlike bulk material, nanocrystalline zinc ferrite consistently displays a partly inverse spinel structure with  $Zn^{2+}$  and  $Fe^{3+}$  ions distributed throughout the A- and B-sites as shown by the given formula [9]:



Where  $\delta$  is the inversion coefficient, which is defined as the fraction of the (A) sites occupied by  $Fe^{3+}$  cations and depends on the crystallite size and the method of preparation.

Sol-gel processing [15], citrate decomposition [16], wet-milling method [14], solid-state reaction [17], hydrothermal crystallization [18], coprecipitation [19], and polymer matrix precipitation [20], were used to create the spinel ferrites.

The current research aims to synthesize, characterize, and evaluate the antioxidant and antibacterial activities of copper ferrite ( $CuFe_2O_4$ ) and zinc ferrite ( $ZnFe_2O_4$ ) nanoparticles.

## 2. Materials and methods

### 2.1. Materials

The analytical-grade chemicals used in this study were obtained from Merk Company which include zinc chloride ( $ZnCl_2$ ), iron chloride hexahydrate ( $FeCl_3 \cdot 6H_2O$ ), ferric nitrate ( $Fe(NO_3)_3 \cdot 9H_2O$ ), copper nitrate ( $Cu(NO_3)_2 \cdot 3H_2O$ ), sodium hydroxide (NaOH), and acetone.

### 2.2. Measurements

The crystallinity and surface morphology of samples were studied by applying Fourier transform infrared spectroscopy (FTIR, Bruker Tensor 27, Bremen, Germany), X-ray diffraction (XRD, Shibuya-ku, Tokyo, Japan) and field emission scanning electron microscope, Energy Dispersive X-Ray analysis (EDX) (MFTIRA III, TESCAN, Czech Republic).

### 2.3. Preparations of zinc ferrite ( $ZnFe_2O_4$ )

An aqueous solution containing 3.3637 g of  $FeCl_3$  and 0.8481 g of  $ZnCl_2$  was dissolved in 50 mL of distilled water to make zinc ferrite. The flask was left in reflux at  $80^\circ C$ , and after 3 hours of strong magnetic stirring, 10% NaOH solution was added to elevate the pH to roughly 10 gradually. The residues from this process were collected, centrifuged, and repeatedly washed with distilled water and acetone before being dried at  $100^\circ C$  under a vacuum for 6 hours. The resultant powders were then calcined at  $450^\circ C$  for 3 hours (**Figure 1**, up scheme).

### 2.4. Preparations of copper ferrite ( $CuFe_2O_4$ )

In 100 mL of distilled water, 0.01 mol of  $Cu(NO_3)_2 \cdot 3H_2O$  and 0.02 mol of  $Fe(NO_3)_3 \cdot 9H_2O$  were dissolved. By adding 10% NaOH, the pH was gradually increased to roughly 10 over three hours of magnetic stirring while the flask was held in reflux at  $80^\circ C$ . The residues produced were collected, centrifuged, and repeatedly washed with acetone and distilled water. The solid was dried for 6 hours at  $100^\circ C$ . The dry material was crushed and then subjected to 3-hour calcination at  $450^\circ C$  (**Figure 1**, down scheme).

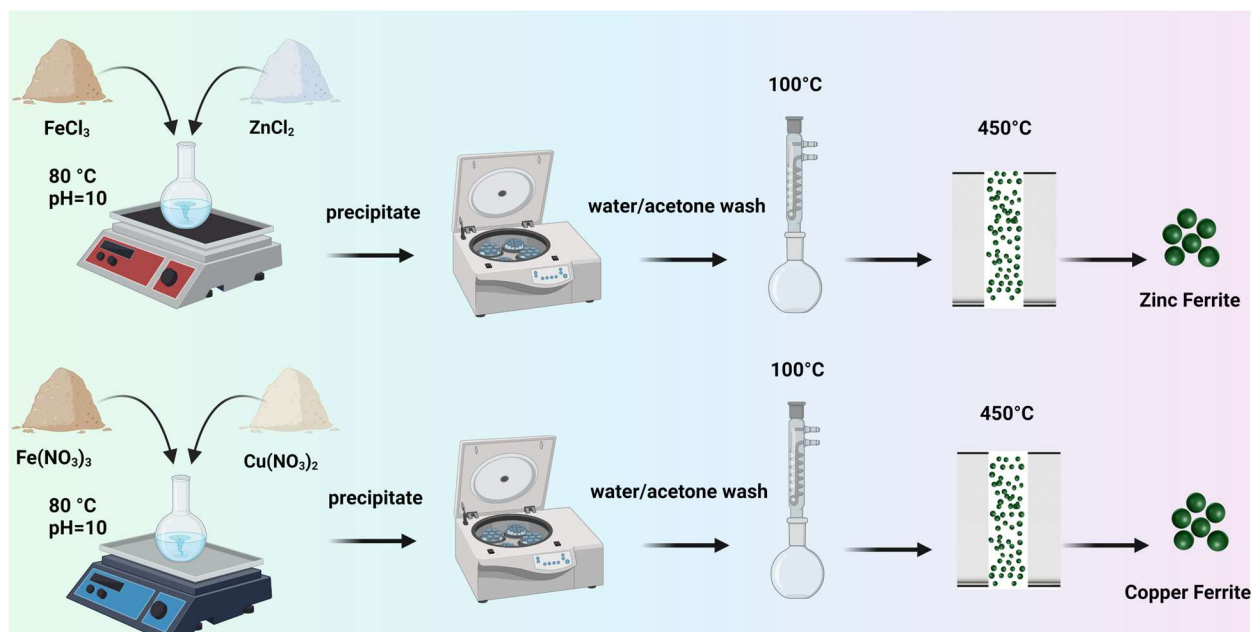


**Figure 1.** A schematic illustration of zinc ferrite (Up) and copper ferrite (Down) preparation by co-precipitation method.

### 2.5. Antioxidant activity

To promote the reaction, 50 mg of  $\text{CuFe}_2\text{O}_4$  or  $\text{ZnFe}_2\text{O}_4$  nanoparticles were introduced to 5 mL of 25 mM DPPH solution and left for 30 minutes at room temperature in dark. The absorbance was then measured at a wavelength of 517 nm using ethanol as a blank [21]. A UV-vis spectrophotometer was used to test the solution's absorbance at 517 nm following filtration. The percentage inhibition of free radicals was calculated based on the formula given below:

$$\text{DPPH inhibition (\%)} = ((A_b - A_s)/A_b) \times 100$$

Where  $A_b$  and  $A_s$  are the ethanolic DPPH absorption (blank) and absorption of the polymer sample solution, respectively [22].

### 2.6. Antibacterial activity

*Escherichia coli* and *Staphylococcus aureus* were used to test the copper ferrite and zinc ferrite nanoparticles' in vitro antibacterial properties. For 24 hours, the infected medium was incubated at 37 °C. 4–6 identical colonies of each microbial strain were injected into tubes containing tryptic soy broth or Muller Hinton broth to examine the antibacterial properties of the produced nanoparticles. For four hours, the infected medium was incubated at 37 °C. At 625 nm, the optical density of every medium was measured after the incubation time. After adjusting the inoculation media's absorbance to 0.08–0.1, a final cell density of around  $1.5 \times 10^8$  CFU/mL was achieved. With the use of a sterile cotton ball, these microbial solutions were applied to the medium. Using DMSO, stock solutions of nanoparticles (20 mg/mL) were created, and PBS (pH 7.2) was used to dilute them. Each nanoparticle (600 mg/mL) was injected into the wells at a volume of 100  $\mu\text{L}$ . The positive controls included penicillin (10  $\mu\text{g}$  per disk), gentamicin (10  $\mu\text{g}$  per disk), sulfamethoxazole (23.75 mg), trimethoprim (1.25 mg), and trimethoprim (5 g per disk). The negative control was achieved by diluting DMSO in PBS. The infected Petri plates were incubated at 4 °C for 3 hours to allow the nanoparticles to disperse into the medium, and then the plates were maintained at 37 °C for 24 hours. Finally, a measurement of the wells' surrounding growth inhibition zones' diameter (millimeters) was made [22].

## 3. Results and discussion

### 3.1. Characterization of zinc ferrite and copper ferrite

**Figure 2** depicts the FTIR spectra of the calcined zinc ferrite and copper ferrite samples. In copper and zinc ferrite, the broadband was seen at  $3428 \text{ cm}^{-1}$  and  $3449 \text{ cm}^{-1}$ , respectively, while absorption maxima at  $1634 \text{ cm}^{-1}$  are attributed to the corresponding hydroxyl group [21]. The symmetry resonance of the  $\text{NO}_3^-$  group is responsible for the

steep peak that can be found in both the spinel ferrites around  $1384\text{ cm}^{-1}$  and  $1394\text{ cm}^{-1}$  [23]. Under  $1000\text{ cm}^{-1}$ , metal oxide vibrations typically occur [23]. At  $797\text{ cm}^{-1}$ , Fe-O-H bending vibrations were recorded [24]. The Fe-O vibration is shown by the small wide band that appears at  $552\text{ cm}^{-1}$  [25].

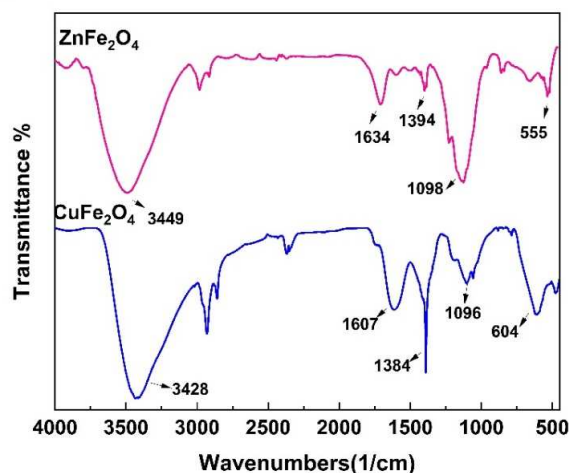


**Figure 2.** The Fourier transform infrared spectra of zinc ferrite ( $\text{ZnFe}_2\text{O}_4$ ) and copper ferrite ( $\text{CuFe}_2\text{O}_4$ ) nanoparticles.

The XRD pattern of the  $\text{CuFe}_2\text{O}_4$  nanoparticles is depicted in **Figure 3A**. The peaks are shown in the  $2\theta$  range of  $18.3^\circ$ ,  $29.9^\circ$ ,  $30.5^\circ$ ,  $34.7^\circ$ ,  $35.8^\circ$ ,  $37.1^\circ$ ,  $41.8^\circ$ ,  $43.7^\circ$ ,  $55.4^\circ$ ,  $57.8^\circ$ ,  $62.1^\circ$ ,  $63.6^\circ$  and  $74.6^\circ$  which corresponds to the reflection plane (101), (112), (200), (103), (211), (202), (004), (220), (105), (321), (224), (400), and (413) respectively [26]. The reflections seen in the X-ray diffraction pattern of zinc ferrite nanoparticles correspond to the (220), (311), (400), (422), (333), (440), and (533) planes, which is proof that the cubic spinel structure was formed [27].

**Figure 3B** shows the vibrating-sample magnetometer (VSM) curves of the copper ferrite and zinc ferrite. The magnetization saturation values of the zinc ferrite and copper ferrite nanoparticles are respectively 16.51 and 21.39 emu/g, demonstrating their magnetic properties.

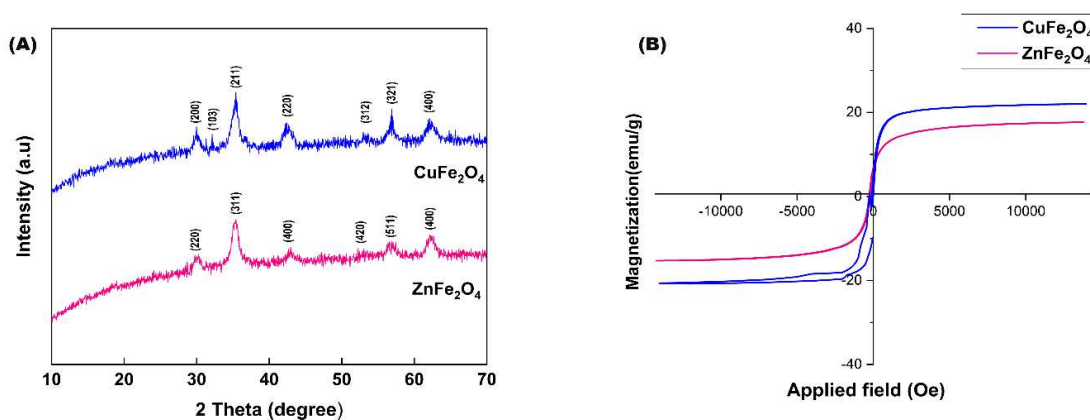


**Figure 3.** (A) X-ray diffraction patterns and (B) vibrating-sample magnetometer curves of zinc ferrite ( $\text{ZnFe}_2\text{O}_4$ ) and copper ferrite ( $\text{CuFe}_2\text{O}_4$ ) nanoparticles.

The chemical makeup of zinc ferrite and copper ferrite was also identified using the EDX method, as seen in **Figures 4A** and **C**. By comparing spectra and tabular data, it was demonstrated that copper ferrite included variable amounts of O, Zn, and Fe elements, as well as that zinc ferrite, contained varying amounts of O, Cu, and Fe elements. **Figures 4B** and **D** display 200 nm-magnification field emission scanning electron microscopy FESEM images of copper ferrite and zinc ferrite, respectively. The FESEM picture revealed an accumulation of zinc ferrite particles with an average

diameter between 20 and 40 nm. Copper ferrite appears as a polyhedron in FESEM images, with very few agglomerations and little porosity. The average diameter of the particles in the copper ferrite was 50 and 100 nm [26].

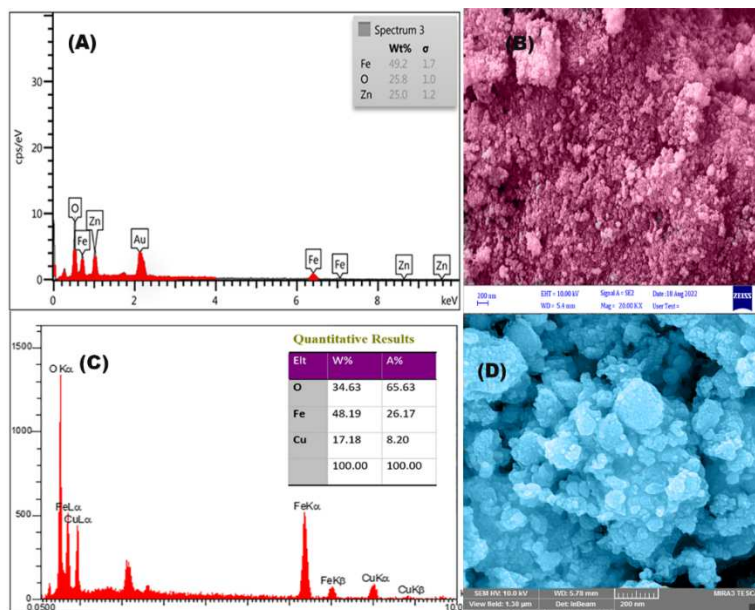


**Figure 4.** Energy dispersive X-Ray spectra (A, C), and field emission scanning electron microscopy (B, D) micrographs of zinc ferrite (ZnFe<sub>2</sub>O<sub>4</sub>) and copper ferrite (CuFe<sub>2</sub>O<sub>4</sub>) nanoparticles respectively.

### 3.2. Antioxidant activities

The importance of the biocompatibility of biomaterials has received much attention due to the effect of oxidative stress that leads to inflammation, chronic diseases, and other problems. For this reason, designing and manufacturing materials with antioxidant properties can play an essential role in increasing biocompatibility. 2,2-diphenyl-1-picrylhydrazyl hydrate (DPPH) free radical scavenging assay method was used to determine the antioxidant activity of CuFe<sub>2</sub>O<sub>4</sub> and ZnFe<sub>2</sub>O<sub>4</sub> nanoparticles. There was no discernible difference in the antioxidant activity of CuFe<sub>2</sub>O<sub>4</sub> and ZnFe<sub>2</sub>O<sub>4</sub> at any of the doses examined. At a concentration of 100 µg/mL, ZnFe<sub>2</sub>O<sub>4</sub> nanoparticles (75.4%) and CuFe<sub>2</sub>O<sub>4</sub> nanoparticles (70.23%) showed the best antiviral activity. The antioxidant activity increased proportionally to higher nanoparticle dosages (Figure 5). This antioxidant activity can be related to the transfer of free electrons from the oxygen atom of nanoparticles to the free radicals present in the nitrogen atom of DPPH molecules. The ability to eliminate free radicals by metal ions with antioxidant effects has been reported in several studies [28]. In addition, in a study, the ZnFe<sub>2</sub>O<sub>4</sub> and CuFe<sub>2</sub>O<sub>4</sub> nanoparticles showed 30.57% ± 1.0% and 28.69% ± 1.14% scavenging activity at 125 µg/mL concentrations [21]. Also, the CuO nanoparticles were fabricated using the fruit and leaf of the *Andean blackberry* (*Rubus glaucus* Benth.). The antioxidant efficacy of the *Andean blackberry* fruit CuO nanoparticles was 89.02%, while 75.92% was achieved for the leaf in the scavenging activity of DPPH radical. Bioactive molecules from the fruit and leaf extracts on the surface of the formed CuO nanoparticles were the main reason for antioxidant effects [29]. Reports of another study showed that CuO nanoparticles at a concentration of 120 mg/mL had 85% DPPH quenching activity [36]. The result of our study is promising and leads to the discovery of CuFe<sub>2</sub>O<sub>4</sub> and ZnFe<sub>2</sub>O<sub>4</sub> nanoparticles as a new source of antioxidants.

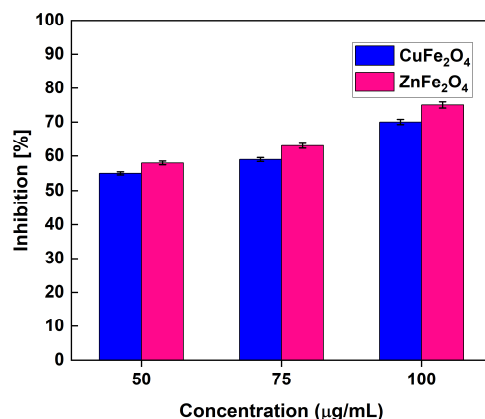


**Figure 5.** Antioxidant activities study of copper ferrite ( $\text{CuFe}_2\text{O}_4$ ) and zinc ferrite ( $\text{ZnFe}_2\text{O}_4$ ) nanoparticles by 2,2-diphenyl-1-picrylhydrazyl hydrate free radical scavenging. Each value is expressed as a mean of  $\pm$  Standard Deviation.

### 3.3. Antibacterial activities

Antibacterial activities were investigated to determine whether disruption of the bacterial cell membrane by  $\text{CuFe}_2\text{O}_4$  and  $\text{ZnFe}_2\text{O}_4$  nanoparticles can lead to the leakage of cytoplasmic substances.

According to the findings in **table 1** and **Figure 6**, *Escherichia coli* and *Staphylococcus aureus* could be killed by  $\text{CuFe}_2\text{O}_4$  and  $\text{ZnFe}_2\text{O}_4$  nanoparticles, respectively.  $\text{ZnFe}_2\text{O}_4$  nanoparticles showed their antibacterial effects to a greater extent in *Escherichia coli* (Gram-negative) bacteria and  $\text{CuFe}_2\text{O}_4$  in *Staphylococcus aureus* (Gram-positive) bacteria. In the bacterial wall of Gram-negative bacteria, a unique arrangement of lipid A, lipopolysaccharides, and peptidoglycans with a thickness of less than 15 nm is seen. While in the structure of gram-positive bacteria, there are mainly very thick peptidoglycans with cell walls that play the role of a boundary to protect proteins so that they can easily leak out when the cell membrane is damaged [2]. Our results showed that  $\text{CuFe}_2\text{O}_4$  and  $\text{ZnFe}_2\text{O}_4$  nanoparticles treatment can cause membrane disruption in both Gram-negative and Gram-positive strains, and can lead to bacterial death through cell membrane damage.

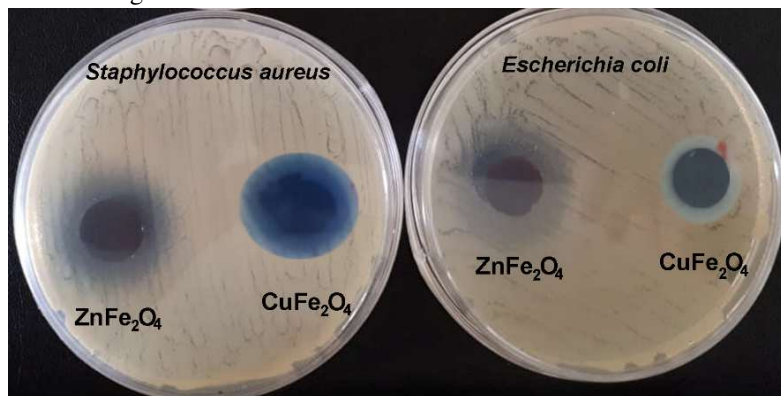


**Figure 6.** Antibacterial activities of copper ferrite and zinc ferrite nanoparticles against *Escherichia coli* and *Staphylococcus aureus* via Kirby–Bauer disk diffusion technique.

**Table 1.** Antibacterial activities of copper ferrite and zinc ferrite nanoparticles via Kirby–Bauer disk diffusion technique.

Entry	Compound	Inhibition Zone (mm)	
		<i>Staphylococcus aureus</i> Gram-Positive (+)	<i>Escherichia coli</i> Gram-Negative (-)
1	$\text{ZnFe}_2\text{O}_4$	$24 \pm 07$	$27 \pm 1.2$
2	$\text{CuFe}_2\text{O}_4$	$22 \pm 1.8$	$12 \pm 09$

## 4. Conclusions

The copper ferrite and zinc ferrite nanoparticles were prepared via the co-precipitation technique, and FTIR, FESEM, XRD, VSM, and EDX confirmed the results. These nanoparticles' antioxidant and antibacterial activity was evaluated using Agar disk diffusion and DPPH tests. Both zinc ferrite and copper ferrite nanoparticles showed appreciable antioxidant activity of 71% and 80%, respectively. Besides, in vitro analysis showed a high antibacterial activity from the synthesized nanoparticles on *Escherichia coli* and *Staphylococcus aureus*. Consequently, the copper ferrite and zinc ferrite nanoparticles could be further explored as antimicrobial and antioxidant promising agents for various biomedical, industrial, and agricultural applications.

## Authors' contributions

All authors contributed to data analysis, drafting, and revising of the paper and agreed to be responsible for all the aspects of this work.

## Declaration of competing interest

The authors declare no competing interest.

## Funding

This paper received no external funding.

## Data availability

Data will be made available on request.

## References

- [1] A. Moammeri, K. Abbaspour, A. Zafarian, E. Jamshidifar, H. Motasadizadeh, F. Dabbagh Moghaddam, Z. Salehi, P. Makvandi, R. Dinarvand, pH-Responsive, Adorned Nanoniosomes for Codelivery of Cisplatin and Epirubicin: Synergistic Treatment of Breast Cancer, *ACS Appl. Bio Mater.* 5(2) (2022) 675-690.
- [2] R. Haghniaz, A. Rabbani, F. Vajhadin, T. Khan, R. Kousar, A.R. Khan, H. Montazerian, J. Iqbal, A. Libanori, H.-J. Kim, F. Wahid, Anti-bacterial and wound healing-promoting effects of zinc ferrite nanoparticles, *J. Nanobiotechnology* 19(1) (2021) 38.
- [3] P. Makvandi, C.-y. Wang, E.N. Zare, A. Borzacchiello, L.-n. Niu, F.R. Tay, Metal-Based Nanomaterials in Biomedical Applications: Antimicrobial Activity and Cytotoxicity Aspects, *Adv. Funct. Mater.* 30(22) (2020) 1910021.
- [4] S. Shaikh, N. Nazam, S.M.D. Rizvi, K. Ahmad, M.H. Baig, E.J. Lee, I. Choi, Mechanistic Insights into the Antimicrobial Actions of Metallic Nanoparticles and Their Implications for Multidrug Resistance, *Int J Mol Sci* 20(10) (2019).
- [5] F. Ordikhani, N. Zandi, M. Mazaheri, G.A. Luther, M. Ghovvati, A. Akbarzadeh, N. Annabi, Targeted nanomedicines for the treatment of bone disease and regeneration, *Med. Res. Rev.* 41(3) (2021) 1221-1254.
- [6] M. Naghdi, M. Ghovvati, N. Rabiee, S. Ahmadi, N. Abbariki, S. Sojeh, A. Ojaghi, M. Bagherzadeh, O. Akhavan, E. Sharifi, M. Rabiee, M.R. Saeb, K. Bolouri, T.J. Webster, E.N. Zare, A. Zarrabi, Magnetic nanocomposites for biomedical applications, *Adv. Colloid Interface Sci.* 308 (2022) 102771.
- [7] Z.G. Özdemir, M. Kılıç, Y. Karabul, B.S. Mısırlıoğlu, Ö. Çakır, N.D. Kahya, A transition in the electrical conduction mechanism of CuO/CuFe<sub>2</sub>O<sub>4</sub> nanocomposites, *J. Electroceramics* 44(1) (2020) 1-15.
- [8] Shyamaldas, M. Bououdina, C. Manoharan, Dependence of structure/morphology on electrical/magnetic properties of hydrothermally synthesised cobalt ferrite nanoparticles, *J. Magn. Magn. Mater.* 493 (2020) 165703.
- [9] M. Ebrahimi, R. Raesi Shahraki, S.A. Seyyed Ebrahimi, S.M. Masoudpanah, Magnetic Properties of Zinc Ferrite Nanoparticles Synthesized by Coprecipitation Method, *J. Supercond. Nov. Magn.* 27(6) (2014) 1587-1592.
- [10] M. Amiri, M. Salavati-Niasari, A. Akbari, Magnetic nanocarriers: Evolution of spinel ferrites for medical applications, *Adv. Colloid Interface Sci.* 265 (2019) 29-44.
- [11] K.K. Kefeni, B.B. Mamba, Photocatalytic application of spinel ferrite nanoparticles and nanocomposites in wastewater treatment: Review, *Sustainable Materials and Technologies* 23 (2020) e00140.
- [12] G. Shahane, Superparamagnetic Manganese Ferrite Nanoparticles: Synthesis and Magnetic Properties, *J. Nanosci. Nanotechnol.* 1 (2015) 178-182.
- [13] T.F. Marinha, I. Chicinaş, O. Isnard, Structural and magnetic properties of the copper ferrite obtained by reactive milling and heat treatment, *Ceram. Int.* 39(4) (2013) 4179-4186.
- [14] M. Mozaffari, H. Masoudi, Zinc Ferrite Nanoparticles: New Preparation Method and Magnetic Properties, *J. Supercond. Nov. Magn.* 27(11) (2014) 2563-2567.

- [15] M. Atif, S.K. Hasanain, M. Nadeem, Magnetization of sol-gel prepared zinc ferrite nanoparticles: Effects of inversion and particle size, *Solid State Commun.* 138(8) (2006) 416-421.
- [16] D. Thapa, N. Kulkarni, S.N. Mishra, P.L. Paulose, P. Ayyub, Enhanced magnetization in cubic ferrimagnetic  $\text{CuFe}_2\text{O}_4$  nanoparticles synthesized from a citrate precursor: The role of  $\text{Fe}^{2+}$ , *J Phys D Appl Phys.* 43(19) (2010) 195004.
- [17] F. Li, H. Wang, L. Wang, J. Wang, Magnetic properties of  $\text{ZnFe}_2\text{O}_4$  nanoparticles produced by a low-temperature solid-state reaction method, *J. Magn. Magn. Mater.* 309(2) (2007) 295-299.
- [18] A. Phuruangrat, B. Kuntalae, S. Thongtem, T. Thongtem, Synthesis of cubic  $\text{CuFe}_2\text{O}_4$  nanoparticles by microwave-hydrothermal method and their magnetic properties, *Mater. Lett.* 167 (2016) 65-68.
- [19] K. Sathiyamurthy, C. Rajeevgandhi, S. Bharanidharan, P. Sugumar, S. Subashchandrabose, Electrochemical and Magnetic Properties of Zinc Ferrite Nanoparticles through Chemical Co-Precipitation Method, *Chemical Data Collections* 28 (2020) 100477.
- [20] S. Roy, J. Ghose, Mössbauer study of nanocrystalline cubic  $\text{CuFe}_2\text{O}_4$  synthesized by precipitation in polymer matrix, *J. Magn. Magn. Mater.* 307(1) (2006) 32-37.
- [21] S. Kanagesan, M. Hashim, S. AB Aziz, I. Ismail, S. Tamilselvan, N.B. Alitheen, M.K. Swamy, B. Purna Chandra Rao, Evaluation of Antioxidant and Cytotoxicity Activities of Copper Ferrite ( $\text{CuFe}_2\text{O}_4$ ) and Zinc Ferrite ( $\text{ZnFe}_2\text{O}_4$ ) Nanoparticles Synthesized by Sol-Gel Self-Combustion Method, *Appl. Sci.* 6(9) (2016) 184.
- [22] A. Ghahremanloo, E.N. Zare, F. Salimi, P. Makvandi, Electroconductive and photoactive poly(phenylenediamine)s with antioxidant and antimicrobial activities for potential photothermal therapy, *New J. Chem.* 46(13) (2022) 6255-6266.
- [23] S. Kanagesan, M. Hashim, S. Tamilselvan, N.B. Alitheen, I. Ismail, G. Bahmanrokh, Cytotoxic effect of nanocrystalline  $\text{MgFe}_2\text{O}_4$  particles for cancer cure, *J. Nanomaterials* 2013 (2013) Article 165.
- [24] S. Krehula, S. Musić, Influence of Mn-dopant on the properties of  $\alpha\text{-FeOOH}$  particles precipitated in highly alkaline media, *J. Alloys Compd.* 426(1) (2006) 327-334.
- [25] M. Iacob, Sonochemical synthesis of hematite nanoparticles, *Chem. J. Mold.* 10(1) (2015) 46-51.
- [26] F.H. Mulud, N.A. Dahham, I.F. Waheed, Synthesis and Characterization of Copper Ferrite Nanoparticles, *IOP Conf. Ser.: Mater. Sci. Eng.* 928(7) (2020) 072125.
- [27] P. Thandapani, M. Ramalinga Viswanathan, J.C. Denardin, Magnetocaloric Effect and Universal Curve Behavior in Superparamagnetic Zinc Ferrite Nanoparticles Synthesized via Microwave-Assisted Co-Precipitation Method, *Phys. Status Solidi B Basic Res.* 215(11) (2018) 1700842.
- [28] P. Kovacic, R. Somanathan, Nanoparticles: toxicity, radicals, electron transfer, and antioxidants, *Methods Mol Biol* 1028 (2013) 15-35.
- [29] B. Kumar, K. Smita, L. Cumbal, A. Debut, Y. Angulo, Biofabrication of copper oxide nanoparticles using Andean blackberry (*Rubus glaucus* Benth.) fruit and leaf, *J. Saudi Chem. Soc.* 21 (2017) S475-S480.